Available online at www.sciencedirect.com

ScienceDirect

Scripta Materialia 98 (2015) 40–43

Scripta MATERIALIA

www.elsevier.com/locate/scriptamat

Plasticity of a scandium-based nanoglass

Xiao Lei Wang,[a] Feng Jiang,[a,*] Horst Hahn,[b,e] Ju Li,[c,d,*] Herbert Gleiter,[b,e] Jun Sun[a] and Ji Xiang Fang[a,*]

[a]*State Key Laboratory for Mechanical Behavior of Materials, School of Materials Science and Engineering, School of Science, Xi'an Jiaotong University, Shaanxi 710049, People's Republic of China*

[b]*Institute for Nanotechnology, Karlsruhe Institute of Technology (KIT), Karlsruhe 76021, Germany*

[c]*Department of Nuclear Science and Engineering, MIT, Cambridge, MA 02139, USA*

[d]*Department of Materials Science and Engineering, MIT, Cambridge, MA 02139, USA*

[e]*Herbert Gleiter Institute of Nanoscience, Nanjing University of Science and Technology, Nanjing, Jiangsu 210094, People's Republic of China*

Received 28 September 2014; revised 9 November 2014; accepted 9 November 2014
Available online 1 December 2014

The mechanical properties of a $Sc_{75}Fe_{25}$ nanoglass and monolithic metallic glass (MG) with identical chemical composition were investigated by means of nanoindentation tests and quantitative in situ compression tests and tensile tests in a transmission electron microscope. The nanoglass exhibits excellent plastic deformation ability relative to the monolithic MG. It is particularly interesting to find that the 400 nm $Sc_{75}Fe_{25}$ nanoglass exhibits a 15% plastic strain under uniaxial tension. Such a nearly uniform tensile plasticity is unprecedented among MGs of similar sample sizes. The enhanced plasticity of the nanoglass can be attributed to its unique microstructure.

Keywords: Nanoglass; Glass–glass interface; Plasticity; In situ TEM

Nanoglasses, a new type of amorphous material with an inhomogeneous microstructure, were first proposed by Jing et al. in 1989 [1]. So far, nanoglasses have been produced by consolidating nanometer-sized glassy clusters [2], magnetron sputtering using powder targets [3] or electrochemical transformation [4]. The microstructure of nanoglasses consists of nanoscaled (<100 nm) contiguous glassy regions (grains) and glass–glass interfaces (GGIs) between these regions. The GGI is usually about one or several nanometers wide with a locally reduced density relative to the densities in the interior of the glassy grains [2,3,5]. The difference in the density of grains and interfaces induces a bimodal distribution of free volume in the nanoglass [2]. Preliminary investigations have shown that nanoglasses present enhanced catalytic activity [3], different magnetic properties [6], remarkable biocompatibility [7] and ultrastable kinetic behavior [8] when compared with chemically identical monolithic metallic glasses (MGs). These novel features of nanoglasses seem to open the way for new technological applications of MGs. Furthermore, nanoglasses show enhanced plasticity due to multiple shear banding [2,9]. However, the underlying mechanism is not clear, and needs further experimental investigation. In this paper, a $Sc_{75}Fe_{25}$ nanoglass was selected as the model material. It is found that the nanoglass exhibited excellent plastic deformation ability (tensile plasticity in particular) relative to a monolithic MG with identical chemical composition, which usually has zero tensile plasticity. This enhanced plasticity is thought to be due to the unique microstructure of the nanoglass.

The $Sc_{75}Fe_{25}$ nanoglass specimens were produced by inert-gas condensation (IGC) [2], and consist of hard zones (glassy grain of diameter D of ~10 nm) with low free volume and soft zones (GGI ~1 nm thick) with high free volume, and increased potential energy [9]. The structure of the nanoglasses can be tuned by varying the size of the glassy regions or the thickness of the GGIs. A study of the atomic structure of this nanoglass and its structural evolution during annealing can be found in Ref. [2]. For comparison, ribbons of a monolithic MG with an identical chemical composition were prepared by melt-spinning.

The mechanical properties of the present nanoglass were investigated by means of nanoindentations and quantitative in situ compression/tension in a transmission electron microscope (TEM). In small-scale tests, the porosity introduced by IGC can be avoided and the mechanical properties related to the microstructure can be investigated in detail. Nanoindentations were carried out using a nanoindenter (TI950, Hysitron Inc., USA) with a Berkovich indenter. All indentation tests were performed to a peak

* Corresponding authors; e-mail addresses: jiangfeng@mail.xjtu.edu.cn; liju@mit.edu; jxfang@mail.xjtu.edu.cn

http://dx.doi.org/10.1016/j.scriptamat.2014.11.010
1359-6462/

load of 10 mN at different loading rates (10, 100 and 1000 μN s^{-1}).

A set of square taper-free pillars with nominal sizes of 300 nm (for compression tests) and 400 nm (for tensile tests) of a $Sc_{75}Fe_{25}$ nanoglass and of a monolithic MG were fabricated by focused ion beam (FIB) techniques. The 300 nm compressive pillars with a cross-section of square and an aspect ratio of ~2 were fabricated using a FEI Helios NanoLab 600i dual-beam FIB system. The tensile sample gauge was trimmed to approach the designed width (~400 nm), length (~1600 nm) and thickness (~400 nm). In situ experiments were performed inside the chamber of a JEOL JEM-2100F TEM, using a Hysitron PI95 TEM Pico-Indenter with a 2 μm diamond flat punch (for compression tests) or a tungsten grip (for tensile tests) that was fabricated using FIB, under displacement-controlled mode with a constant value 2 nm s^{-1} (nominal strain rate ~1×10^{-3} s^{-1}). The data acquisition rate was about 200 points s^{-1}. The fabrication method and test method of tensile tests is similar to that used by Tian et al. [10].

Figure 1 displays the nanoindentation load–displacement (P–h) curves for the nanoglass as well as for the monolithic MG. Only the loading portions of the P–h curves are shown. The origin of each P–h curve has been displaced for clarity. Usually, the P–h curves of MGs are segmented due to numerous discrete bursts of rapid displacements at nearly constant load (Fig. 1a), while at various loading rates, no bursts of rapid displacement were observed in the curves of the nanoglass (Fig. 1b). These behaviors (discrete bursts of rapid displacements) are analogous to the serrated flow that has been reported for various MGs in compression tests [11]. Each serration corresponds to the nucleation and growth of one shear band. With increasing loading rate, the serrated flow changes from small step-like P–h curves (at low rates) to relatively smooth curves. This change agrees with the observations reported for various MGs such as in Pd–Ni–P and Mg–Cu–Gd [12]. The absence of discrete bursts of rapid displacements in the P–h curves suggests that the nanoglass might deform uniformly by numerous shear bands being activated simultaneously. The deformation features noted at the free surfaces of the nanoglass and monolithic MG under plastic indentation can be seen in the insets of Figure 1a and b, respectively. The shape of the indent observed in the nanoglass is similar to that observed in ductile materials with material pileup mounds near the indent, whereas the indent shape of the MG appears to be similar to that in brittle materials.

In order to investigate the processes involved in the deformation of the nanoglass in comparison to the monolithic MG, quantitative in situ compression tests and tensile

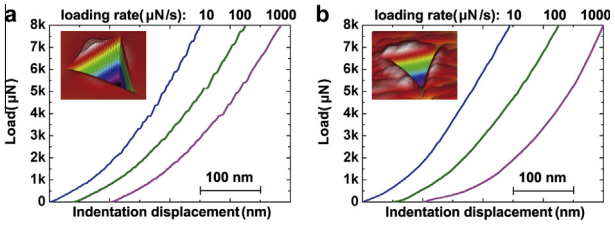

Figure 1. Typical load–displacement (P–h) curves measured at different loading rates for (a) $Sc_{75}Fe_{25}$ monolithic MG, and (b) $Sc_{75}Fe_{25}$ nanoglass. The insets of (a) and (b) are the SPM surface features for monolithic MG and nanoglass after nanoindentation, respectively.

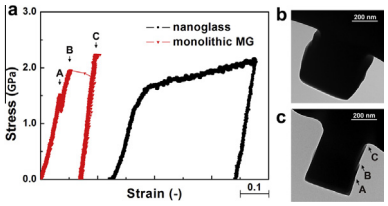

Figure 2. (a) The compressive stress–strain curves of the nanoglass and the monolithic MG; post-mortem TEM pictures of (b) nanoglass pillar and (c) monolithic MG pillar.

tests were performed for both the nanoglass and the monolithic MG in a TEM. The compressive stress–strain curves are shown in Figure 2a. In the case of the 300 nm nanoglass, the initial linear elastic deformation was followed by a plastic yield. As the plastic deformation process went on, the stress increased to ~1.27 GPa and no large stress drops were observed until the test was stopped at a pre-selected strain of 50%. Numerous small stress drops with amplitudes of <0.1 GPa were noted during the deformation of the nanoglass. Although not every shear band can be identified in the movie, these stress drops should originate from the propagation of a large number of smaller shear bands [11]. It is suggested that the nanoglass sample deformed uniformly due to multiple shear band mechanism rather than localized shear. The plastic strain was ~43% in the axial direction and ~35% in the transverse direction (Fig. 2b). The monolithic MG pillar exhibited purely elastic behavior until a stress drop with an amplitude of ~0.3 GPa occurred while the stress goes up to ~1.53 GPa (corresponding to the burst at point A in Fig. 2a). This stress drop was correlated with an obvious shear offset appearing on the free surface of pillar (point A in Fig. 2c), followed by another catastrophic stress drops (point B in Fig. 2a and c). The entire deformation processes of two samples can be found in the online Supplementary Information (Movies 1 and 2, respectively).

The tensile stress–strain curves of the nanoglass and the monolithic MG are shown in Figure 3a. The nanoglass deformed like a ductile material. It displayed significant plasticity after the yield point and before final failure. The entire tension process can be seen in Movie 3. Numerous small shear banding events corresponding to small stress drops in stress–strain curves can be seen during the deformation of the nanoglass. Whether or not the plastic deformation counts as uniform depends on the time/load/spatial resolutions of the instrument [13].

Several snapshots from this movie are displayed in Figure 3c. These snapshots correspond to points 1–6 on the stress–strain curve. At the beginning of the deformation process, the stress–strain relationship was linear. The nanoglass yielded at a stress of ~1.3 GPa and at a strain of 5.2%. Subsequently it softened and continued to undergo plastic deformation. After a uniform plastic deformation of about 6.2% (total strain 11.4% at point 4), an obvious necking in the gauge length appeared. Finally, a total strain of 18% was obtained when the in situ tensile test was stopped at a pre-selected tensile displacement. After unloading, elastic deformation recovered and a plastic strain of 15.6% was retained. The scanning electron microscopy (SEM) image of the as-deformed sample revealed the formation of a gradual neck in the gauge length due to the significant plastic deformation as shown in Figure 3d. The enlarged SEM image indicated a plastic strain of at least 15% in the axial